Cyclic coding for Brillouin optical time-domain analyzers using probe dithering

HARITZ IRIBAS,[1] ALAYN LOAYSSA,[1,3] FLORIAN SAUSER,[2] MIGUEL LLERA,[2] AND SÉBASTIEN LE FLOCH[2,4]

[1]*Institute of Smart Cities, Universidad Pública de Navarra, Campus Arrosadia s/n, 31006 Iruñea, Spain*
[2]*HE-ARC, Rue de la Serre 7, 2610 Saint Imier, Switzerland*
[3]*alayn.loayssa@unavarra.es*
[4]*sebastien.lefloch@he-arc.ch*

Abstract: We study the performance limits of mono-color cyclic coding applied to Brillouin optical time-domain analysis (BOTDA) sensors that use probe wave dithering. BOTDA analyzers with dithering of the probe use a dual-probe-sideband setup in which an optical frequency modulation of the probe waves along the fiber is introduced. This avoids non-local effects while keeping the Brillouin threshold at its highest level, thus preventing the spontaneous Brillouin scattering from generating noise in the deployed sensing fiber. In these conditions, it is possible to introduce an unprecedented high probe power into the sensing fiber, which leads to an enhancement of the signal-to-noise ratio (SNR) and consequently to a performance improvement of the analyzer. The addition of cyclic coding in these set-ups can further increase the SNR and accordingly enhance the performance. However, this unprecedented probe power levels that can be employed result in the appearance of detrimental effects in the measurement that had not previously been observed in other BOTDA set-ups. In this work, we analyze the distortion in the decoding process and the errors in the measurement that this distortion causes, due to three factors: the power difference of the successive pulses of a code sequence, the appearance of first-order non-local effects and the non-linear amplification of the probe wave that results when using mono-color cyclic coding of the pump pulses. We apply the results of this study to demonstrate the performance enhancement that can be achieved in a long-range dithered dual-probe BOTDA. A 164-km fiber-loop is measured with 1-m spatial resolution, obtaining 3-MHz Brillouin frequency shift measurement precision at the worst contrast location. To the best of our knowledge, this is the longest sensing distance achieved with a BOTDA sensor using mono-color cyclic coding.

© 2017 Optical Society of America

References and links

1. T. Horiguchi, K. Shimizu, T. Kurashima, M. Tateda, and Y. Koyamada, "Development of a distributed sensing technique using Brillouin scattering," J. Lightwave Technol. **13**(7), 1296–1302 (1995).
2. M. Alem, M. A. Soto, and L. Thévenaz, "Analytical model and experimental verification of the critical power for modulation instability in optical fibers," Opt. Express **23**(23), 29514–29532 (2015).
3. S. M. Foaleng, F. Rodríguez-Barrios, S. Martín-López, M. González-Herráez, and L. Thévenaz, "Detrimental effect of self-phase modulation on the performance of Brillouin distributed fiber sensors," Opt. Lett. **36**(2), 97–99 (2011).
4. L. Thévenaz, S. F. Mafang, and J. Lin, "Effect of pulse depletion in a Brillouin optical time-domain analysis system," Opt. Express **21**(12), 14017–14035 (2013).
5. A. Domínguez-López, X. Angulo-Vinuesa, A. López-Gil, S. Martín-López, and M. González-Herráez, "Non-local effects in dual-probe-sideband Brillouin optical time domain analysis," Opt. Express **23**(8), 10341–10352 (2015).
6. T. Shimizu, K. Nakajima, K. Shiraki, K. Ieda, and I. Sankawa, "Evaluation methods and requirements for the stimulated Brillouin scattering threshold in a single-mode fiber," Opt. Fiber Tech. **14**(1), 10–15 (2008).
7. Y. Dong, L. Chen, and X. Bao, "Extending the sensing range of Brillouin optical time-domain analysis combining frequency-division multiplexing and in-line EDFAs," J. Lightwave Technol. **30**(8), 1161–1167 (2012).
8. A. Zornoza, R. A. Pérez-Herrera, C. Elosúa, S. Díaz, C. Bariain, A. Loayssa, and M. López-Amo, "Long-range hybrid network with point and distributed Brillouin sensors using Raman amplification," Opt. Express **18**(9), 9531–9541 (2010).
9. X. Angulo-Vinuesa, S. Martín-López, J. Nuño, P. Corredera, J.D. Ania-Castañón, L. Thévenaz, and M. González-Herráez, "Raman-assisted Brillouin distributed temperature sensor over 100 km featuring 2 m resolution and 1.2°C

uncertainty," J. Lightwave Technol. **30**(8), 1060–1065 (2012).

10. J. Urricelqui, M. Sagues, and A. Loayssa, "Brillouin optical time-domain analysis sensor assisted by Brillouin distributed amplification of pump pulses," Opt. Express **23**(23), 30448–30458 (2015).

11. J. J. Mompó, J. Urricelqui, and A. Loayssa, "Brillouin optical time-domain analysis sensor with pump pulse amplification," Opt. Express **24**(12), 12672–12681 (2016).

12. M. A. Soto, G. Bolognini, F. D. Pasquale, and L. Thévenaz, "Long-range Brillouin optical time-domain analysis sensor employing pulse coding techniques," Measurement Sci. Technol. **21**(9), 094024 (2010).

13. M. Taki, Y. Muanenda, C. J. Oton, T. Nannipieri, A. Signorini, and F. D. Pasquale, "Cyclic pulse coding for fast BOTDA fiber sensors," Opt. Lett **38**(15), 2877-2880 (2013).

14. S. Le Floch, F. Sauser, M. Llera, and E. Rochat, "Novel Brillouin optical time-domain analyzer for extreme sensing range using high-power flat frequency-coded pump pulses," J. Lightwave Technol. **33**(12), 2623–2627 (2015).

15. S. Le Floch, F. Sauser, M. Llera, M. A. Soto, and L. Thévenaz, "Colour simplex coding for Brillouin distributed sensors," Proc. SPIE **8794**, 879437 (2013).

16. M. A. Soto, G. Bolognini, and F. D. Pasquale, "Analysis of pulse modulation format in coded BOTDA sensors," Opt. Express **18**(14), 14878–14892 (2010).

17. Z. Yang, M. A. Soto, and L. Thévenaz, "Increasing robustness of bipolar pulse coding in Brillouin distributed fiber sensors," Opt. Express **24**(1), 586–597 (2016).

18. R. Ruiz-Lombera, J. Urricelqui, M. Sagues, J. Mirapeix, J. M. López-Higuera, and A. Loayssa, "Overcoming non-local effects and Brillouin threshold limitations in Brillouin optical time-domain sensors," IEEE Photonics J. **7**(6), 1–9 (2015).

19. A. Minardo, R. Bernini, and L. Zeni, "A simple technique for reducing pump depletion in long range distributed Brillouin fiber sensors," IEEE Sensors J **9**(6), 633–634 (2009).

20. A. Dominguez-Lopez, Z. Yang, M. A. Soto, X. Angulo-Vinuesa, S. Martín-López, L. Thévenaz, and M. González-Herráez, "Novel scanning method for distortion-free BOTDA measurements," Opt. Express **24**(10), 10188–10204 (2016).

21. F. Wang, C. Zhu, C. Cao, and X. Zhang, "Enhancing the performance of BOTDR based on the combination of FFT technique and complementary coding," Opt. Express **25**(4), 3504–3513 (2017).

22. M. A. Soto and L. Thévenaz, "Modeling and evaluating the performance of Brillouin distributed optical fiber sensors," Opt. Express **21**(25), 31347–31366 (2013).

1. Introduction

Distributed optical fiber sensors based on Brillouin optical time-domain analysis (BOTDA) [1] have been widely employed due to their capability to provide high accuracy in distributed measurements of temperature or strain. The basic principle of this technique consists in acquiring the Brillouin frequency shift (BFS) of every position in the fiber, as a result of the interaction between a pump pulse with a counter-propagating continuous wave probe through stimulated Brillouin scattering (SBS) [1]. Some of the practical scope of applications of this technology are in the monitoring of oil and gas pipelines, railway inspection, assessment of high voltage cables, fire detection, and many other structural health monitoring applications.

Several of these applications require a large sensing range. However, the sensing range of BOTDA sensors is limited by the signal-to-noise ratio (SNR) that can be achieved at the receiver. Thus, the sensing range of BOTDA sensors is fundamentally limited by the attenuation suffered by the pump and probe waves along the optical fiber, which eventually makes the measured signal to be too small to be properly detected with the required SNR. This drawback could be overcome by increasing the power of the pump and/or the probe waves. Nevertheless, the maximum pump pulse power that can be injected in the fiber is limited by the onset of non-linear effects such as modulation instability [2] or self-phase modulation [3]. Moreover, the maximum probe power that can be deployed is also limited by the appearance of the so-called non-local effects [4, 5] and noise induced by spontaneous Brillouin scattering [6].

In order to overcome these limitations, and achieve an improvement of the SNR of BOTDA sensors, a number of techniques have been proposed. A first possibility is to amplify the pulses by the use of erbium-doped fiber amplifiers (EDFA) as pulse repeaters along the fiber link [7]. However, this technique needs a power supply for the in-line EDFAs, which is inconvenient for its real applicability. It is also possible to make use of Raman amplification [8, 9] or distributed Brillouin pump amplification [10, 11] to alleviate the effects of fiber attenuation on the probe

wave, on the pump wave or on both of them.

Another alternative to enhance the SNR of BOTDA sensors is the use of different coding techniques, such as mono-color simplex coding [12], mono-color cyclic coding [13] and color-coding [14, 15], which have proved to be useful for long sensing range analyzers. Nevertheless, all these coding techniques require a compromise between the deployed fiber length and the probe and pump power that can be brought into the fiber in order to avoid undesired effects that distort the decoding of the measurement. Some of the issues related to the use of pulse coding in BOTDA sensors that have been studied or mentioned before are the need for pulse trains in non-return-to-zero modulation format [16], the effects of power fluctuation of the coded pulses [12, 15] or the detrimental effects resulting from pump depletion [17].

In this work, we demonstrate a BOTDA sensor that combines probe dithering and cyclic coding. We have recently introduced probe-dithered BOTDA sensor in which wavelength modulation of the probe is used to mitigate non-local effects and increase the Brillouin threshold of the fiber link [18]. Thus, a larger probe wave power can be injected in the fiber, increasing the SNR of the sensor, The additional use of mono-color cycling coding, with its associated coding gain, further increases the performance. However, as higher power levels are used, several limitations related to coding become significant. Specifically, we analyze the distortion in the decoding process, and the errors in the measurement that this distortion introduces, due to three factors: the power difference of the successive pulses of a sequence, the appearance of pump pulse depletion due to non-local effects and the non-linear amplification that results when using mono-color cyclic coding. Finally, the results of this analysis is deployed to demonstrate an improved long-range BOTDA setup.

2. Fundamentals of dithered-probe BOTDA sensor with cyclic coding

The fundamentals of the BOTDA sensor using probe dithering are schematically described in Fig. 1, where the optical waves involved in the technique are depicted. As it is highlighted in Fig. 1(a), the optical frequency of the probe waves is modulated following a saw-tooth shape [11], an alternative would be to use a triangular shape, which has been shown to have a similar effect [18]. Additionally, this frequency modulation (FM) is synchronized to the pump pulses so that a pulse sequence experiences the same wavelength of the probe waves at any given location. In this setup second-order non-local effects [5] are prevented because the FM modulation of the probe waves makes the Brillouin interaction upon the optical pulse to spread over a large frequency range, leading to a broadening of the effective gain and loss spectra induced by both probes on the pump: these spectra mutually compensate to avoid any distortion of the pulse spectrum [18]. Moreover, the FM increases the Brillouin threshold limit of the fiber, thus reducing the effective amplification of spontaneous Brillouin scattering in the fiber, so that the probe power can overtake the Brillouin threshold limit. Therefore, a very large probe power can be deployed to enhance the SNR in detection. Furthermore, as it is depicted in Fig. 1(b), the FM of the probe wave is used to perform the scan of the Brillouin spectra, instead of doing it by a conventional frequency sweep: at every location in the fiber the probe wave is made to interact with additional frequencies of the Brillouin spectrum simply by changing the relative delay between the probe wave FM modulation and the pump pulse [11, 18], as it is depicted schematically in Fig. 1(b). The number of relative delays is given by the relation between the peak-to-peak frequency deviation (Δf) and the desired frequency step (δ), being the same than in a conventional BOTDA scheme. Notice that this scanning method does not introduce any measurement time penalty compared to the conventional frequency sweep. Finally, in order to retrieve the Brillouin gain spectrum (BGS) of the fiber, a reorder of the acquired data has to be done. The aim of this processing is to compensate the frequency shift introduced to the probe wave at each location due to the FM modulation. For that purpose, a simple shift is applied to the elements of the columns of the matrix containing the probe wave samples (rows) for each
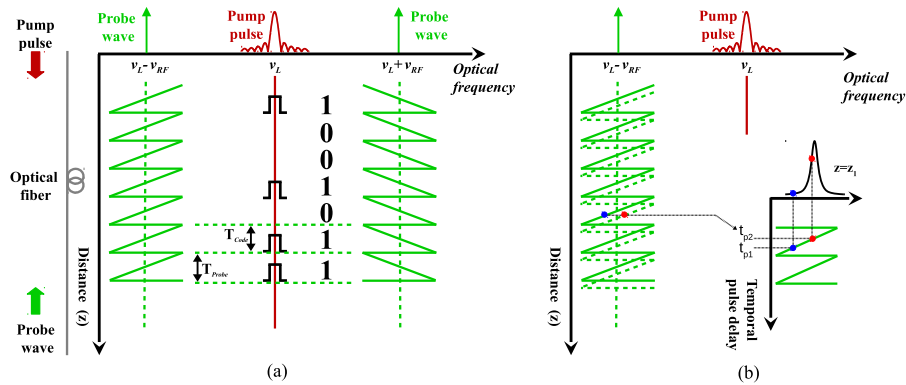
Fig. 1. Fundamentals of the technique

relative delay between the FM modulation and the pump pulses [18].

In order to further increase the SNR, we combine the probe dithering technique with mono-color cyclic coding. For this purpose, we introduce a code based on a circulant matrix of dimension L_c, with L_c a prime number [14]. The code is generated following the recurrence equation for an integer n:

$$\begin{cases} u_1 = 0 \\ u_{n+1} = (u_n + n) \; mod \; L_c \end{cases} \tag{1}$$

where mod is the modulo function and $n \in [1, \frac{L_c+1}{2}]$. The position p_n of the consecutive "1" bits for the first line of the code matrix is simply given by the relation: $p_n = u_n + 1$. The first line of the code matrix for a code length of seven is represented in Fig. 1(a). The improvement of the SNR given by the coding gain is the same as for simplex coding, i.e., $(L_c + 1)/2\sqrt{L_c}$, with the advantage of a reduced measurement time: as the code scheme is cyclic, there is no need to repeat each sequence that corresponds to a line of the coding matrix. In this way, the first sequence is simply repeated in a continuous loop, providing fast averaging. Moreover, the number of possible code lengths using this recurrence equation can be chosen between any prime number, in contrast to conventional code generation techniques where the code length has to be a number given by $2n - 1$, n being an integer. Note that in order to properly decode the signal, the period of the FM modulation of the probe waves has to be equal to the code period ($T_{probe} = T_{code}$), i. e., the temporal distance between two of the contiguous bits of the generated cyclic code. In addition, in a cyclic code all codewords of a sequence must fit simultaneously inside the fiber. Therefore, for a given fiber length, the code period, together with the FM modulation period, needs to be modified depending on the code length. Finally, to properly decode the signal and retrieve the BGS of the fiber, the frequency shift of the probe waves must be compensated by reordering the decode matrix, as it has been previously explained.

An important consideration when using mono-color cyclic coding in BOTDA sensors is related of the limitations faced regarding the maximum pump and probe power that can be injected in a given fiber sensing link. In the following, we analyze these limitations in the context of our probe-dithered BOTDA sensor with mono-color cyclic coding. Furthermore, most of the considerations made are equally valid for other BOTDA configurations, although the detailed analysis and comparison of the relative severity of the various impairments in each setup is outside the scope of this paper.

The first limitation in pump and probe power that our probe-dithered BOTDA sensors with

mono-color cyclic coding face comes from the onset of non-local effects, due to pump pulse depletion, which introduce an error in the measurement decoding process. Previous works have shown that for conventional BOTDA setups without coding the pump pulse depletion is directly linked to the probe power injected in the fiber [4]. Thus, the pump pulse power at the output of the fiber is given by the expression (assuming a BOTDA in a gain configuration):

$$P_P(L) = P_P(0) \, exp(-\alpha L) \, exp\left(\frac{-g_B(\Delta v)}{A_{eff}} P_{CW}(L) \, L_{eff}\right) \tag{2}$$

where $L_{eff} \equiv (1 - exp(-\alpha L))/\alpha$ is the effective length, with L the length of the fiber, A_{eff} is the effective area of the sensing fiber, $P_P(0)$ is the pulse power at the input of the fiber and $P_{CW}(L)$ is the input probe power at the far end of the fiber link. However, Eq. (2) is no longer valid when using mono-color cyclic coding because the successive pulses interact with a probe wavefront that has been already amplified by previous pulses. Therefore, the amount of pump depletion suffered by the single-pulses, instead of being just related to the power of the probe wave injected in the fiber, as given by Eq. (2), also depends on the amplification of the probe wavefronts by previous pulses in the coded sequence. Hence non-local effects will appear earlier in BOTDA setups using mono-color pump pulse cyclic coding than in conventional single-pulse BOTDA sensors. Furthermore, even for a dual-probe wave BOTDA configuration, which mitigates non-local effects [19, 20], the presence of multiple pulses in the fiber when using mono-color cyclic coding makes pump depletion to become significant at lower input probe wave power than for single-pulse dual-probe systems. In fact, all BOTDA setups deploying mono-color cyclic coding are affected by pump depletion, but the amount of pump depletion will be different for each configurations. Our probe-dithered BOTDA makes the sensor more robust to pump depletion in comparison to other BOTDA configurations, due to the FM of the probe wave. Finally, another assumption regarding non-local effects that becomes invalid for BOTDA system with mono-color cyclic coding is the independence of pump depletion on pump pulse power that is conveyed by Eq. (2). In a BOTDA system with mono-color cyclic coding, the higher the pump pulse power, the larger the amplification of the probe wave by previous pulses in a sequence, and hence, the larger the depletion of a particular pump pulse. Therefore, non-local effects in BOTDA sensors with mono-color cyclic coding lead to the need to reduce the probe power as well as the pump pulse power compared to the sensor without coding, which is counterproductive for the sensor performance.

The second limitation for pump and probe powers in BOTDA sensors with mono-color cyclic coding comes from the fact that coding techniques can only be applied to linear interactions. However, in BOTDA interactions, the Brillouin gain experienced by the probe wave does not depend linearly on the pump pulse power, but exponentially. Indeed, the variation in the continuous wave (CW) probe signal power, ΔP_{CW}, detected in the receiver at a given instant, t, due to a SBS gain interaction at a location z_i along the fiber with a pump pulse is given by:

$$\Delta P_{CW}(t, \Delta v) = P_{CW}(L) \, exp(-\alpha L) \, [G_i(t, \Delta v) - 1] \tag{3}$$

where α is the fiber attenuation, L is the fiber length, Δv is the local detuning of the probe wave frequency from the center of the Brillouin spectrum and $G_i(t, \Delta v)$ is the Brillouin gain defined as follows,

$$G_i(t, \Delta v) = exp\left[\int_{z_i}^{z_i + \Delta z} \frac{g_B(\Delta v)}{A_{eff}} P_P(0) \, exp(-\alpha z_i) \, dz\right] \equiv exp(g_i) \tag{4}$$

where Δz is the spatial resolution given by the pulse duration and g_B is the local Brillouin gain coefficient for a given Δv frequency shift. Only assuming that the Brillouin gain is very

small ($g_i \ll 1$), can Eq. (3) be simplified considering that the BOTDA sensor operates in a small signal regime:

$$G_i(t, \Delta\nu) \approx 1 + \int_{z_i}^{z_i+\Delta z} \frac{g_B(\Delta\nu)}{A_{eff}} P_P(0) \, exp(-\alpha z_i) \, dz = 1 + g_i \tag{5}$$

Hence, the Brillouin gain in a single-pulse BOTDA configuration can be approximately considered to depend linearly on the gain provided by a single pulse so that in principle linear optical pulse coding techniques could be applied. Nevertheless, the total amount of gain that the probe wave experiences in a BOTDA deploying coding is provided by interaction with all the pulses in the sequence for the whole codeword, so that ΔP_{CW} is obtained as follows:

$$\Delta P_{CW}(t, \Delta\nu) = P_{CW}(L) \, exp(-\alpha L) \, [G_T(t, \Delta\nu) - 1] \tag{6}$$

where $G_T(t, \Delta\nu)$ is the total Brillouin gain provided by the successive pulses, which is given by:

$$G_T(t, \Delta\nu) = G_1 G_2 G_3 ... G_{L_c} = exp\left(\sum_{i=1}^{L_c} gi\right) \approx 1 + \sum_{i=1}^{L_c} gi \tag{7}$$

where $G_i = exp(g_i)$ is the gain provided by each pulse with position i in the coded sequence. In order for mono-color cyclic coding to be applicable, the approximation in the last equality term of Eq. 7 needs to be valid so that the total gain experienced by the probe wave is the linear superposition of the gains provided by each pulse. However, this requires the total Brillouin gain induced by the pump pulses sequence on the probe needs to be relatively small ($\sum_{i=1}^{L_c} gi \ll 1$), which is much more difficult because, despite the fact that the individual gains provided by each pulse may be small, the accumulated gain provided by the many pulses in a long pulse sequence becomes much larger. Thus, in order to avoid distortion, it becomes necessary to reduce the gain induced by each individual pulse by further limiting the pump power below the thresholds imposed by the onset of nonlinear effects such as modulation instability.

Finally, coding techniques are limited by the fact that for most of them, so as to decode properly the signal, it is mandatory that all coded pump pulses have the same power. This indirectly limits the pump power due to the transient behavior of the erbium-doped fiber amplifiers (EDFA) that are typically deployed to amplify the pulses before injecting them in the fiber. This transient behavior worsens for large input powers making the pump pulses in a sequence to experience different gain.

All these limitations lead to a trade-off between the maximum pump and probe powers that can be used in mono-color cyclic coding systems and the sensor performance/measurement error. The need to reduce pump and/or probe power implies a reduction of the effective SNR enhancement that the application of coding potentially brings. In fact, there may be configurations of the BOTDA setup in which the SNR decrement due to the limited pump and probe power could completely counteract the enhancement brought by coding. Based on these considerations, mono-color cyclic coding is really more useful in long-range loop configurations, where only half of the fiber is used for the sensing while the other half is used as a leading fiber to take the probe wave to the remote end of the sensing link. In this configuration the probe power injected in the long-length leading fiber is limited to the Brillouin threshold of that fiber; hence, the power finally reaching the end of the leading fiber and being injected into the sensing fiber is reduced. Fortunately, the loop configuration is the one deployed in most long-range sensing systems on the field. However, as it has been mentioned above, our technique for probe dithering serves to increase the effective Brillouin threshold of the leading fiber, hence the probe power that can reach the sensing fiber can still be sizable, leading to an improvement

of the SNR. Moreover, as it has been explained, the use of dithered-probe waves makes the sensor more robust to pump depletion, so that higher pump and probe powers can be injected in the fiber. Therefore, the use of a dithered-probe wave alleviates the limitation caused by the cascade effect of pump depletion due to the interaction between the probe wave with multiple pulses. Thus, leading again to an enhancement of the SNR.

It is important to point out that different coding techniques presented so far in the literature will be affected differently by the presented impairments. For instance, color coding [14, 15] could alleviate the limitation regarding non-linear amplification, while three-tone bipolar coding technique [17] could get rid of non-linear amplification and reduce the impact of pump depletion, but at the cost of a great increase in setup complexity.

3. Experimental setup

In order to evaluate the power limitations of mono-color cyclic coding and to demonstrate the capabilities of the proposed technique, a BOTDA setup following the scheme in Fig. 2 was assembled. The optical source was a 1550-nm DFB laser, whose output was divided by a coupler into two branches. In the lower branch of the setup, a dual-probe wave was generated using a Mach-Zehnder electro-optic modulator (MZ-EOM). This modulator was driven by an arbitrary waveform generator (AWG), and biased for minimum transmission so as to generate a FM-modulated double-sideband suppressed-carrier signal. For this purpose, the AWG provides a microwave signal with an instantaneous frequency varying around the Brillouin frequency shift (BFS) of the fiber following a saw-tooth shape. Then, an EDFA was used to amplify the probe wave power level. Finally, before the receiver, a tunable narrow-band fiber Bragg grating (FBG) was used to filter out one of the probe sidebands and the Rayleigh backscattering originating from the pump wave.
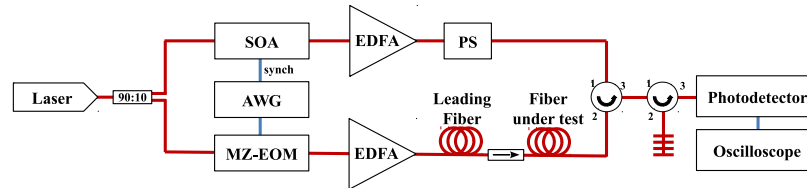

Fig. 2. Experimental setup for the BOTDA sensor.

In the upper branch, so as to generate a pump pulse with a high extinction-ratio (ER), the pump signal was pulsed by a semiconductor optical amplifier (SOA), with an ER up to 50 dB. The AWG was used to generate the coding pulse sequences, and also to synchronize them with the FM modulation of the probe waves. Then, the pump pulse power was amplified in another EDFA, and to smooth polarization effects in the Brillouin interaction along the fiber, the polarization state of the pulsed pump was randomized with a polarization scrambler before being launched into the sensing fiber.

4. Evaluation of the power limits for cyclic coding

A 25 km length of standard single-mode fiber (ITU G.652) was used initially to evaluate the limits on the probe and pump power that can be injected in the fiber when using mono-color cyclic coding before the appearance of distortions and measurement errors in the decoded signal. The FM modulation of the saw-tooth of the probe waves was changed for different code lengths, so as to maintain the same slope of the saw-tooth shape for all the measurements. Thus, as for different code lengths the code period was different, in order to satisfy the condition explained in
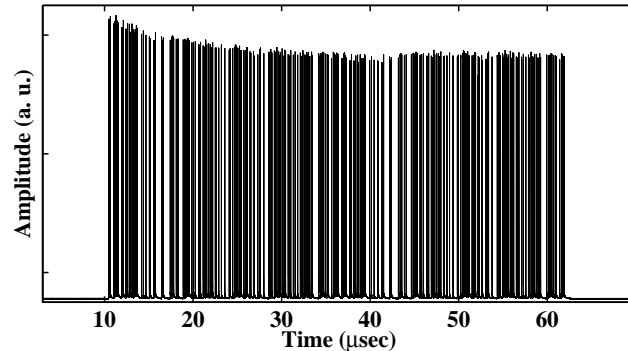
Fig. 3. Power measurement of the cyclic pulse train of the first sequence for $L_c = 263$

section 2, the peak-to-peak frequency deviation of the FM modulation was changed for different code lengths. The probe power was fixed to -7 dBm per sideband at the input of the fiber, so as to simulate the maximum probe power that could be obtained at the fiber-under-test (FUT) in a 200 km loop configuration. That probe power was obtained by subtracting the attenuation of the 100 km leading fiber (approximately 20 dB) from the maximum power that can be injected in the fiber due to the Brillouin threshold with probe-dithering (approximately 13 dBm per sideband). Finally, the pump wave was modified in terms of pulse duration, pulse power and code length.

First, the effect of power variations among the different pulses of the coded sequences was investigated. A sequence of 20-ns pulses with a code length of $L_c = 263$ was used. In order to make sure that there was no pulse depletion, the pump pulses were first amplified to 19 dBm by an EDFA and then reduced by an attenuator to 13 dBm power. Figure 3 depicts the power of the pulses in the sequence that clearly shows a non-flat response, due to the transient behavior of the EDFA. If this is not taken into account during the decoding process, the obtained measurement will be distorted with rapid variations of an acquisition trace, as it is highlighted in Fig. 4(a). In order to retrieve an undistorted smooth signal, as in Fig. 4(b), pulse power fluctuations have to
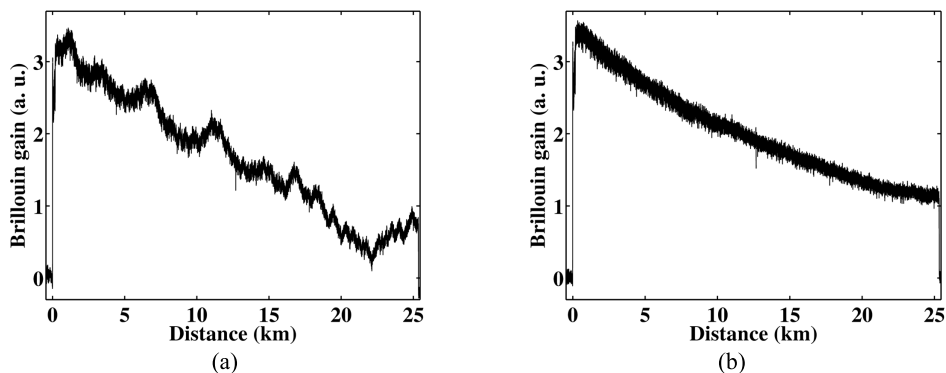

Fig. 4. Decoded BOTDA trace at BFS of the fiber for a pulse of 13 dBm power and 20 ns; (a) without taking into account the pulse power variations and (b) taking into account the pulse power variations
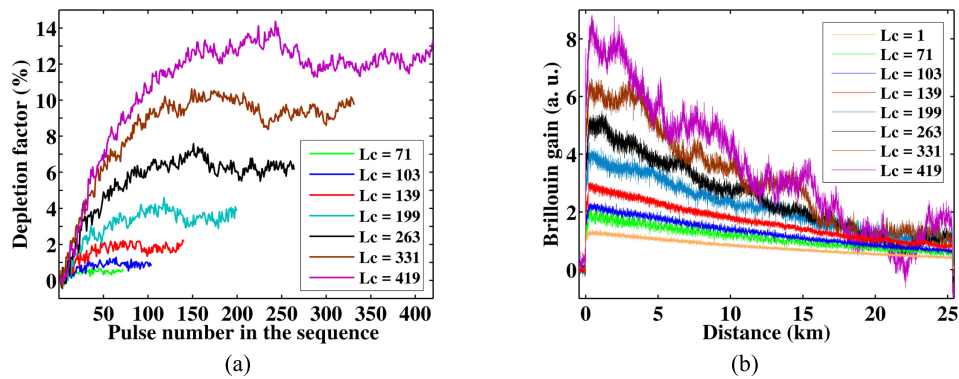
Fig. 5. For a pulse of 19 dBm power and 20 ns; (a) Depletion of the pulses of the sequence for different code lengths (b) distortion in BOTDA trace due to pulse depletion for different code lengths

be corrected, and therefore, each "1" of the original coding matrix has to be actually replaced by the weighted pulse power, which needs to be monitored by another detector [15]. Note that this effect is reduced, if not completely suppressed, by repeating the coded sequence in a continuous way, so that the EDFA has a more linear behavior.

We also analyzed the distortion in the decoded signal produced by pump depletion due to non-local effects. For this purpose, the power level of the pulse was raised to 19 dBm, while the pulse duration was maintained at 20 ns. Figure 5(a) portrays the pump depletion factor that the successive pulses of a cyclic sequence suffer for different code lengths. It can be observed that even with the FM modulation of the probe waves, which makes the system less affected by non-local effects than a conventional double-probe BOTDA system and for a relatively short code length of $L_c = 71$ there is already a small depletion in the pulses (smaller than 1%). Moreover, note that the depletion suffered by each pulse of a sequence is not the same, increasing accordingly with the amplification of the probe wave by previous pulses. Indeed, it can be observed that the depletion of the pulses is a cascade effect, since the depletion factor of the nth pulse would be affected by the amplification suffered by the probe wave for all the coding units before (1st to $n\text{-}1^{\text{th}}$). However, notice that in Fig. 5(a) a given code unit experiences a different depletion factor depending on the total code length, this is due to the fact that, as it was explained before, the code period needs to be modified as a function of the code length. For larger code lengths, the code period is reduced and this leads to stronger overall pump depletion.

Figure 5(b) depicts the decoded BOTDA trace at the BFS of the sensing fiber for different code lengths. Notice that the difference in depletion factor for the successive pulses of a code sequence has an analogous distortion effect on the decoded traces to those due to amplitude variations of the pulses induced by the transient effects in the EDFA highlighted in Fig. 4(a). This is reasonable, considering that the difference in deflection induces a difference in pulse amplitude. The figure also shows that the larger the pulse depletion of the pulses of the sequence, the higher the distortion. Furthermore, even for a small pulse depletion, e.g., for a code length of $L_c = 139$, in which a maximum depletion factor of approximately 2% is reached, there is a small distortion in the decoding process that is more visible at the end of the BOTDA trace. Note that some traces of Fig. 5(b) are noisier than they should, for instance, for $L_c = 71$. This anomaly is attributed to the polarization scrambler deployed, which was found to change slightly the time-averaged degree of polarization that it generated over time, probably due to heating.
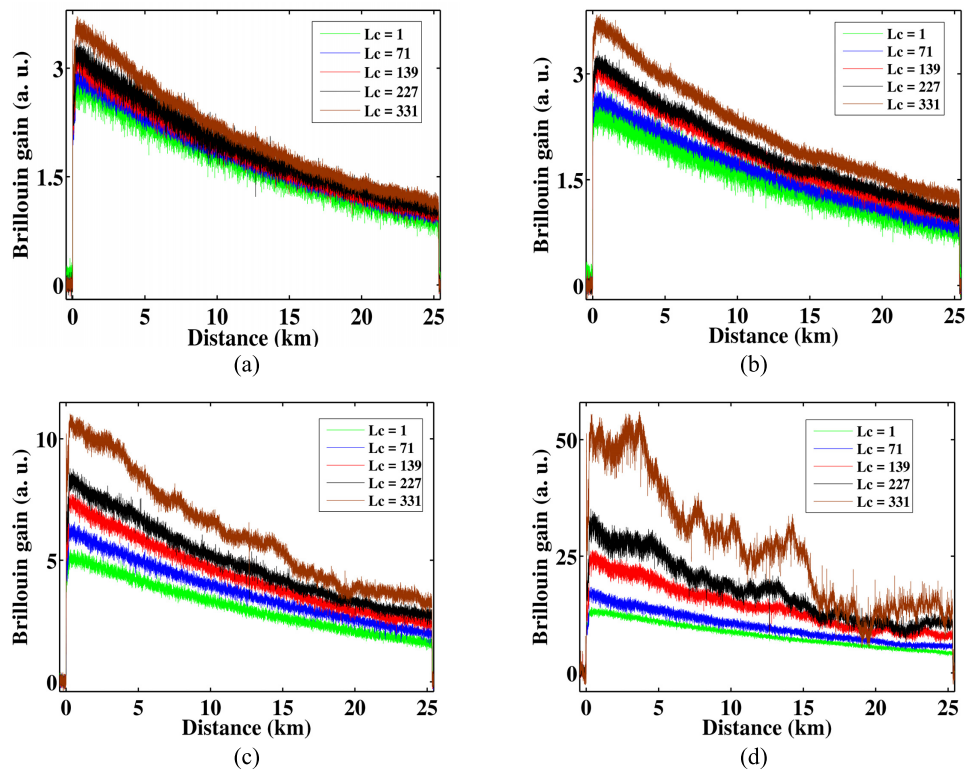
Fig. 6. Obtained BOTDA trace at BFS of the fiber for a pulse of (a) 13 dBm and 20 ns, (b) 16 dBm and 10 ns, (c) 16 dBm and 20 ns and (d) 16 dBm and 40 ns

Additionally, we studied the non-linear amplification of the signal due to the code length. In a purely linear interaction, the amplitude of the decoded BOTDA trace should be the same for all code lengths. However, Fig. 6 highlights the different amplitudes of the decoded BOTDA trace due to the non-linear amplification measured while scanning the peak of the Brillouin gain spectrum. The non-linear amplification was studied as a function of the code length, pulse duration and pulse power. As it can be seen, the amplitude of the decoded BOTDA traces increases with the code length, resulting in measurement distortion. Furthermore, this distortion is also frequency-depend because for frequencies further away from the peak of the Brillouin gain spectrum (BFS of the fiber), the gain provided by the pump pulses to the probe wave will be so small that the linear interaction condition will be fulfilled. Notice also that as it was expected, the non-linear amplification effects increase with increasing pulse duration (more gain to the probe due to increased interaction length) and power. The additional distortion in the form of rapid variations of the signal in the decoded traces in Fig. 6 can be attributed to the appearance of pulse depletion due to non-local effects already visualized in Fig. 5(b). In any case, it is important to clarify that, as non-local effects and non-linear amplification occur both at same time, the distortion in the form of rapid variations of the trace could be a consequence of both, considering that they can both reinforce each other.

Figure 7 summarizes the non-linear amplification effect by depicting the normalized amplitude in percentage value of the beginning of the decoded BOTDA trace (entry point of the pump pulses) for different code lengths. To normalize the amplitude, for each of the different pulse duration and power, the amplitude value of a single pulse is used as a reference. It can be seen
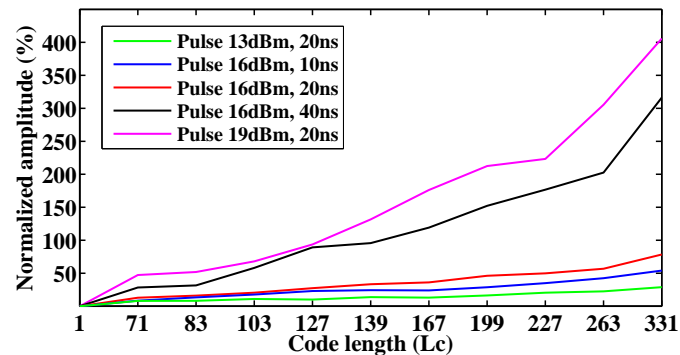
Fig. 7. Non-linear amplification for different code lengths, and different pulse power and duration

that for low pulse power the non-linearity of the gain interaction can not be clearly discerned for small code lengths, but in the case where code length, pulse power or duration is higher, the non-linear regime becomes noticeable. Thus, it is clear that the non-linear amplification has a direct link to the pump power, the code length and also to the pump duration.

Finally, in order to analyze the error in the measurement that all these distortions introduce, distributed temperature measurements were performed. The pulse power was set to 19 dBm and the duration was set to 20 ns, corresponding to approximately 2 m spatial resolution. The traces were averaged 1000 times. The final meters of the fiber were placed loose in a climatic chamber with a fixed temperature, while the rest of the fiber was held at room temperature in a spool. The BFS along the fiber was calculated by performing a quadratic fit on the measured Brillouin gain spectra. Figure 8 depicts the evolution of the measured BFS at the end of the fiber for different code lengths and for a single-pulse measurement. The heated section is clearly visible, and the measured BFS of the single-pulse measurement agrees with the smaller code length measurements, while for the others the error increases. Specifically, it can be observed that for $L_c = 1$ to $L_c = 103$ there is no significant error while for $L_c = 139$ and $L_c = 199$ the error in the measured hot spot are 2.2 MHz and 4 MHz respectively. Which makes sense, since the greater the distortion the larger the error. Therefore, the error increases for a longer code
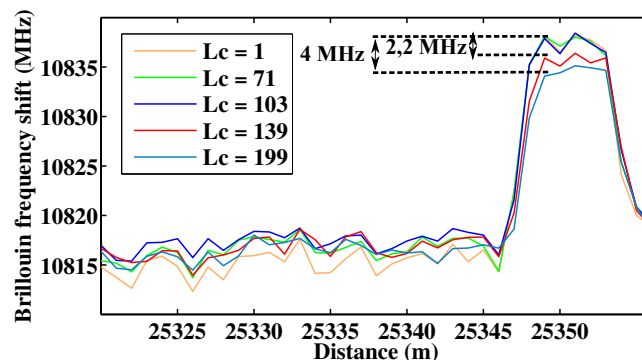

Fig. 8. Calculated BFS as a function of distance at the final locations of the fiber, with a fix temperature for different code lengths

length. For all of these reasons, in order to avoid distortions in the decoded signal, that leads to an error in the precision of the analyzer, it is mandatory to reduce the pump power, the probe power, the code length or the pump duration, which can lead, in several cases, to a non-existing improvement of the SNR of the analyzer.

5. Performance of the dithered-probe BOTDA sensor with cyclic coding

Once the limitations of mono-color cyclic coding were studied, and in order to analyze the ultimate performance of our BOTDA sensor combining cyclic coding and probe dithering, distributed temperature measurements were performed over a loop of 164 km length of standard single-mode (ITU G.652) fiber. The pulse duration was set to 10 ns, corresponding to approximately 1-m spatial resolution, and the code length was set to $L_c = 79$, which was found to be the largest code length that could be used without the appearance of the previously analyzed impairments in mono-color cyclic coding, without decreasing the power of the optical waves, which would lead to a decrease SNR. In this case, the code period was 10.7 μs. Thus, in order to satisfy the requirement explained in section 2, the FM of the probe waves was set to a period of 10.7 μs and peak-to-peak frequency deviation of 250 MHz. The final meters of the fiber were placed loose in a climatic chamber, while the rest was held at room temperature in a spool.
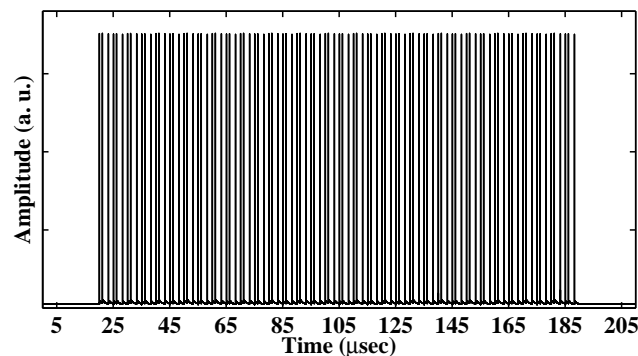

Fig. 9. Power measurement of the cyclic pulse train of the first sequence for $L_c = 79$

The probe wave was boosted to 15 dBm, so that there was 12 dBm per sideband, by a conventional EDFA before being injected in the 82-km leading fiber, so that at the input of the sensing fiber the probe power was -1.8 dBm. This value was measured to be the maximum tolerable value before the appearance of noise induced by spontaneous Brillouin scattering. In addition, we did not observe any other effect that deteriorated the performance of the sensor like for instance four-wave mixing. Note that in a conventional BOTDA, the Brillouin threshold limits the maximum probe power that can be injected into the fiber to approximately 6 dBm. Hence, the use of the probe-dithering method entails an intrinsic enhancement in SNR. The pulse power was amplified to 20 dBm, a level close to the limit before modulation instability becomes significant, by a specific EDFA (Nano-second Pulsed EDFA, Amonics) for generating pulses, so as to generate a flat power pulse train of the codeword as it is highlighted in Fig. 9. The performance of this EDFA was also checked with different code periods and lengths, obtaining an equally flat response free from transient effects. In this case, the decoding process is simplified, with no need for an additional detector to measure the power of the sequence of pulses injected in the fiber. In case that this special EDFA is not available, the supplementary detector would be deployed to monitor the pump pulses, or other alternative technique to suppress the transients of the EDFA could be used [21].
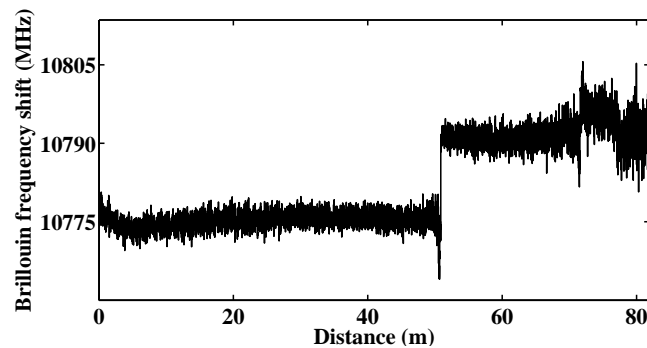
Fig. 10. Distribution of the BFS profile of the sensing fiber

The setup in Fig. 2 was completed by adding an EDFA preamplifier before the receiver. This EDFA was placed between two tunable narrow-band FBGs that were used to filter out one of the probe sidebands and the Rayleigh backscattering originating from the pump wave. In addition, the final FBG served to limit the ASE noise being detected.

In order to analyze the measurement precision of the sensor, a series of 10 consecutive measurements in stable temperature conditions were performed. For that purpose, the final 5 km of the fiber was placed in a climatic chamber at constant temperature. From these measurements, the uncertainty of the BFS measurement was found to be 3 MHz (1-σ) at the end of the fiber under test. Figure 10 portrays the BFS along the whole sensing fiber, where four fiber spools are clearly distinguishable, with a fairly uniform BFS in all of them. Note that the BFS along the fiber was calculated by performing a simple quadratic fit on the BGS. Furthermore, the frequency step of the spectral scan was 2.3 MHz and 16000 averages were used to obtain the final traces.
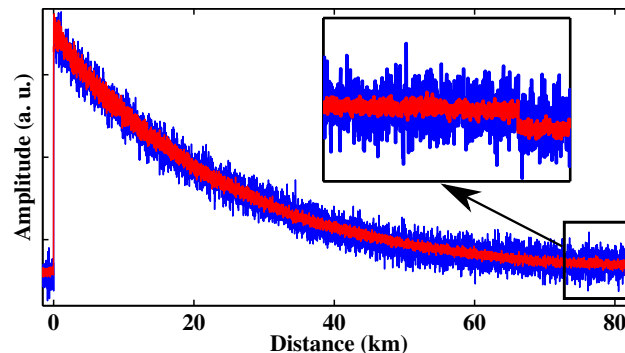

Fig. 11. BOTDA traces at BFS obtained for the analyzer with a 79-bit cyclic coding (red) and without aplying coding (blue)

The noise reduction effect provided by the coding technique can be clearly appreciated in Fig. 11, which compares a conventional BOTDA trace with another one obtained after decoding. The measured SNR enhancement was 6.2 dB, in good agreement with the theoretical expected value (6.5 dB) for a 79-bit code length. The code length was limited by the appearance of the distortion studied in section 4 for longer lengths.
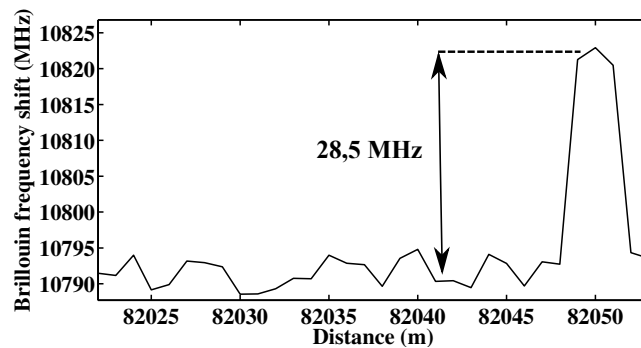
Fig. 12. Calculated BFS as a function of distance at the final locations of the fiber, with the last 3 meters in a climatic chamber

Finally, we introduced in a climatic chamber the last 3 m of the sensing fiber while the rest of the fiber was placed at room temperature in spools. The difference between the room temperature and the climatic chamber was set to 27°C. Figure 12 depicts the obtained BFS at the far end of the FUT, where the hot spot can clearly be observed, with a difference of 28.5 MHz between the hot spot and the ambient temperature, which perfectly matches with the expected value. Furthermore, based on the obtained results, the figure-of-merit (FoM) of this BOTDA setup was calculated [22], obtaining a value of 7,100.

6. Conclusion

In this paper, we have presented a study on the practical limitations on probe and pump power in a BOTDA sensor that uses mono-color cyclic coding. In particular, we have studied the distortion and the error that corrupts the measurement because of three factors: the power fluctuations of the pulse sequence, the appearance of pump depletion and the non-linear amplification of the probe wave resulting from mono-color cyclic coding. We reach to the conclusion that, in order to avoid errors in the decoded signal, there is a compromise between the maximum pump and probe powers that can be injected in the fiber, the code length, the pump pulse duration and the fiber length. Thus, the use of coding techniques is limited to cases in which the obtained coding gain has a real benefit in the measurement in comparison with a single-pulse configuration. This corresponds to high sensing ranges in loop configurations.

In addition, we have introduced an enhanced BOTDA analyzer that combines mono-color cyclic coding and a frequency modulated dual-probe wave configuration. The capabilities of the technique have been analyzed by performing distributed temperature measurements over a 164 km loop length of fiber with high precision (3 MHz) and spatial resolution (1 m). After a correct adjustment of the sensor parameters, the effective code gain corresponding to the used code length (L_c = 79) is in good agreement with the theoretical value, thus proving the usefulness of the combined techniques. To the best of our knowledge, this is the longest sensing distance achieved with a BOTDA sensor using mono-color cyclic coding.